

Research Article

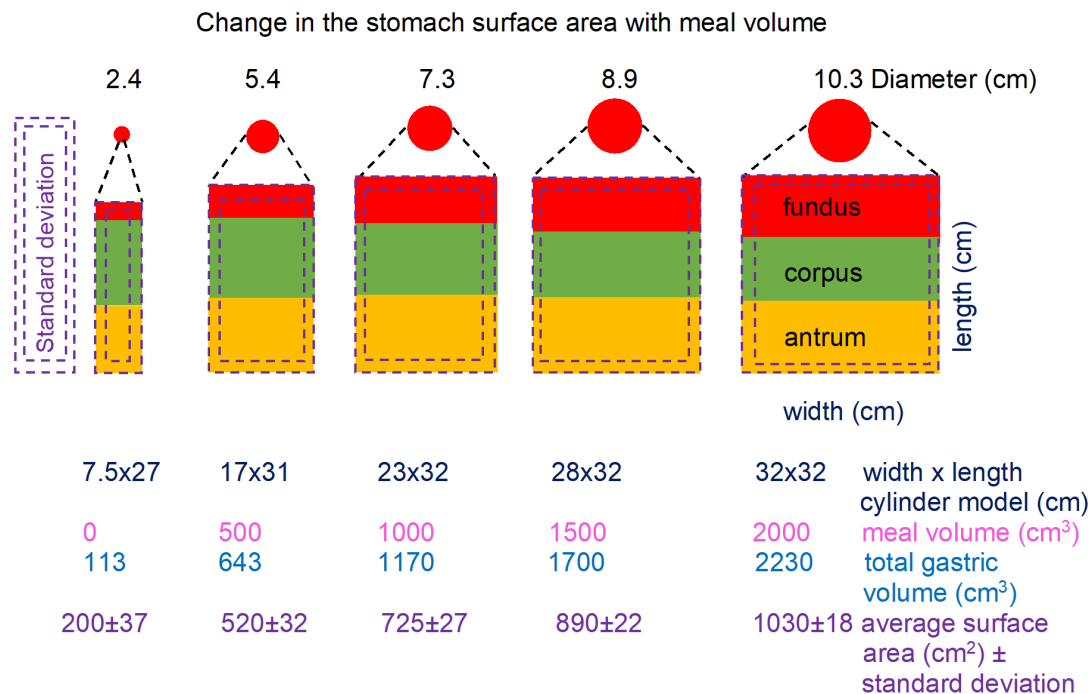
Surface area values for the human stomach including changes in length and diameter or width with meal volume

Thomas Hurr¹

1. Independent researcher

To quantify the amount of solid, liquid or gas that can be adsorbed on to a surface, the surface area must be known. Equations were developed to calculate the macroscopic surface area of the adult human stomach in vivo, at any given meal volume. For a meal volume of $V \approx 0-2000 \text{ cm}^3$, the surface area $SA \approx 113-1030 \text{ cm}^2$ and by using a cylinder-shaped stomach model, the diameter $D \approx 2.4-10.3 \text{ cm}$, length $L \approx 27-32 \text{ cm}$ and width $W \approx 7.5-32 \text{ cm}$. The cylinder model found for a given volume, the standard deviation in average surface area values may result from fluctuations in both length, diameter and width, indicating the stomach, by changing shape, changes surface area.

Corresponding author: Thomas Hurr, tomhurr15@gmail.com



The in vivo changes in the stomach average diameter, width, length and macroscopic surface area with standard deviation values, including 3 stomach regions, with meal volume. Using a cylinder model, the diameter is shown as a top view of the fundus region which is then un-rolled together with the cylinder caps and flattened to form a rectangle of width and length. Data adapted from Bertoli et al. 2023 ^[1].

Keywords: stomach surface area, stomach size, stomach volume, stomach diameter, stomach length.

Introduction

Knowledge of the SA of the human stomach and the SA of solid food consumed during a meal, can allow quantification of liquid or solid adsorption on both surfaces, for comparative studies ^[2]. An in vivo magnetic resonance imaging (MRI) study of 12 healthy volunteers determined the SA of the human stomach, at baseline and on consuming 500 cm³ of soup, also reporting that no standard reference values of SA could be found in the literature ^[1]. A typical meal has a meal volume (V_M) of $V_M \approx 1000 \text{ cm}^3$ with a maximum $V_M \approx 1500 \text{ cm}^3$ ^[3]. This report adapts and extends the numerical SA and V data from the MRI study to generate equations that estimate the SA for any V_M and by using a cylinder model for the stomach, calculate changes in length (L) and width (W) on consumption or digestion ^[1]. A cylinder model

is used as some stomachs are reported to be cylindrical in shape and has less complex geometry than the more common J shape. In a study of the stomachs from 50 adult cadavers, 58% had a J shape, 20% cylindrical, 14% crescentic and 8% reverse L [4]. In another study with 24 adult cadavers and 46 post-mortem specimens, 71% of stomachs had a J shape, 7% cylindrical, 7% crescentic and 15% reverse L [5]. Models of digestion processes generally refer to the more common J shape [3][6].

Results and Discussion

Calculation of the surface area for all meal volumes and 3 compartmental regions of the stomach

From a MRI study [1], after consuming a meal with $V_M \approx 500 \text{ cm}^3$, it was found the stomach contained a total liquid volume (V_L) with standard deviation (SD) of $V_L \approx 516(30) \text{ cm}^3$ and so it is assumed:

$$V_L \approx V_M \quad (1)$$

Total gastric volume (V_T) includes both V_L , gas (V_G) and the stomach wall (V_W) such that:

$$V_T \approx V_L + V_G + V_W \quad (2)$$

At baseline or pre-meal, $V_T \approx 140(32) \text{ cm}^3$, higher than $V_L \approx 39(23) \text{ cm}^3$ and $V_G \approx 27(14) \text{ cm}^3$ combined, presumably due to the influence of V_W [1]. Values for V and SA include the wall thickness of the stomach, resulting in lower internal SA values at lower meal volumes, with reducing influence, due to gastric distention, at higher meal volumes. Stomach wall thickness has been reported as 2.6-5.1(0.6) mm ex vivo with different thicknesses depending on the stomach regions as fundus, corpus and antrum [7]. The V_T values were measured at baseline and on consumption of the soup at 5 intervals 0, 15, 30, 45 and 60 minutes with the amount of gas showing a relatively constant value of $V_G \approx 98(56)$ - $109(55) \text{ cm}^3$ [1]. The SA and V_T and V_L values determined after the consumption of soup are assumed to be the same values as if food had just been consumed, rather than declining values from digestion, over time [1]. The line of best fit between V_T and V_L , with SD values included, shows a linear equation (eq.):

$$V_T \approx 1.06V_L + 113\text{cm}^3 \quad (3)$$

with SD values either added or subtracted to the V_T or V_L values (V_T+SD/V_L , V_T-SD/V_L , V_T/V_L+SD , V_T/V_L-SD) or both added or both subtracted (V_T+SD/V_L+SD , V_T-SD/V_L-SD) resulting in 6 possible combinations per V_T/V_L pair and an additional 36 values, Figure 1A [1]. The value for the gradient of 1.06 shows an

almost equal rate of increase of V_T with V_L . From eq. (3), $V_M \approx V_L = 0 \text{ cm}^3$, before a meal had begun, $V_T \approx 113 \approx V_G + V_W$.

The change in gastric SA and V_T , with SD values included as described previously for V_L and V_T , show a line of best fit, Figure 1B:

$$SA \approx 14.9V_T^{0.5496} \quad (4)$$

Equation (4) can be used to calculate the change in $SA \approx 200\text{--}1032 \text{ cm}^2$ for $V_M \approx 0\text{--}2000 \text{ cm}^3$, using eqs (1) and (3) from the $V_T \approx 113\text{--}2233 \text{ cm}^3$ values, Table 1. The SD in the SA values can be added (or subtracted) from the average SA values, showing a line of best fit, Figure 1C:

$$SA(+SD) \approx 0.99SA + 37 \text{ and } SA(-SD) \approx 1.01SA - 37 \quad (5)$$

Equation (5) can be used to calculate the SD in the SA values and is shown for $SA \approx 0\text{--}2000 \text{ cm}^2$, with the largest SD values at low V_M or V_L , Figure 1C, Table 1.

An in vitro ultrasonography study with 8 adults reported a single value for the inner stomach $SA \approx 196 \text{ cm}^2$ and $V \approx 277 \text{ cm}^3$, showing a SA/V ratio similar to that for a sphere, which has the minimum possible SA/V ratio, Figure 1B [8]. Normalized gastric compartmental SA and V_T data for the fundus, corpus and antrum are also shown using values from the MRI study for $V_T \approx 140\text{--}669 \text{ cm}^3$ extended using power eqs. to $V_T \approx 0\text{--}2000 \text{ cm}^3$, Figure 2 [11].

A cylindrical model showing changes in length and width on consumption or digestion

Taking the square root of known or calculated SA values from eq. (4) gives values for length (L) and width (W) as $L \times W$ where $L=W$ as $SA \approx \sqrt{200}\text{--}\sqrt{1032} \approx 14 \times 14 \text{ cm} - 32 \times 32 \text{ cm}$ for $V_M \approx 0\text{--}2000 \text{ cm}^3$. To determine changes in the L and W of the stomach where L may not necessarily be equal to W, with changes in V_M , a cylindrical model to describe the stomach shape was used. Geometric shapes like spheres or cylinders have a V and SA defined by their radius (r) and height (h) from well-known equations such that for the volume of a sphere (V_S):

$$V_S = (4\pi r^3)/3 \quad (6)$$

and SA of a sphere (SA_S):

$$SA_S = 4\pi r^2 \quad (7)$$

For cylinder volume (V_C):

$$V_C = \pi r^2 h \quad (8)$$

and cylinder SA (SA_C):

$$SA_C = 2\pi r^2 + 2\pi r h \quad (9)$$

with $h=L$ and diameter (D) as $D=2r$.

A comparison of the SA/V_T values from the MRI study with those calculated for a cylinder (eqs. (8), (9)) with $L=3D$, $6D$, $9D$ shows $L\approx 9D$ intersects with the experimental values at low meal volumes, changing to $L\approx 6D$ at $V_T\approx 600 \text{ cm}^3$ to $L\approx 3D$ at $V_T\approx 2000 \text{ cm}^3$, Figure 1B [1]. For example, if $L=6D=12r$ then from eq. (8), $V=\pi r^2 h=12\pi r^3$ and from eq. (9) $SA=2\pi r^2 + 24\pi r^2=26\pi r^2$ to generate the SA_C/V_T curves, Figure 1B.

From the MRI study [1], the 6 experimental V_T and SA values with an additional 36 values by including the SD, as described earlier, can be used in eqs. (8), (9) and solved simultaneous for h (L) and r ($D=2r$), with negative, imaginary numbers and values with $D>L$ neglected, Figure 3A. From eq. (8), for a given V_T value, a range of possible cylinder L and D values and therefor SA (eq. (9)) values are possible. For a specific V_T and SA value, only one L and D value can be calculated from simultaneous equations where $L>D$. The solution to the simultaneous equations shows scattered L and D values due to the SD in V_T and SA , possibly the result of volume changes during digestion. Variations in the SA may also be the result of variations in the stomach L and D during digestion, indicated by many of the experimentally determined SA values closely aligned to the lines showing possible L/D values at any given V_T , Figure 3A. The standard deviation in average surface area values may result from fluctuations in both length and diameter, rather than be an error of measurement.

The range of possible SA values for $V_T=140 \text{ cm}^3$, where the SD values are included, are shown with $SA\approx 193\text{--}246 \text{ cm}^2$ for $L\approx 18\text{--}32.3 \text{ cm}$ and $D\approx 2.3\text{--}3.2 \text{ cm}$, Figure 3A. A change in shape at a constant V , may provide the stomach some control over SA and presumably the adsorption rates of gastric components, with more tube-like shapes ($L>D$ for example $L=9D$) increasing SA while more spherical shapes ($D\approx L$ for example $L=3D$) decreased SA , Figure 1B.

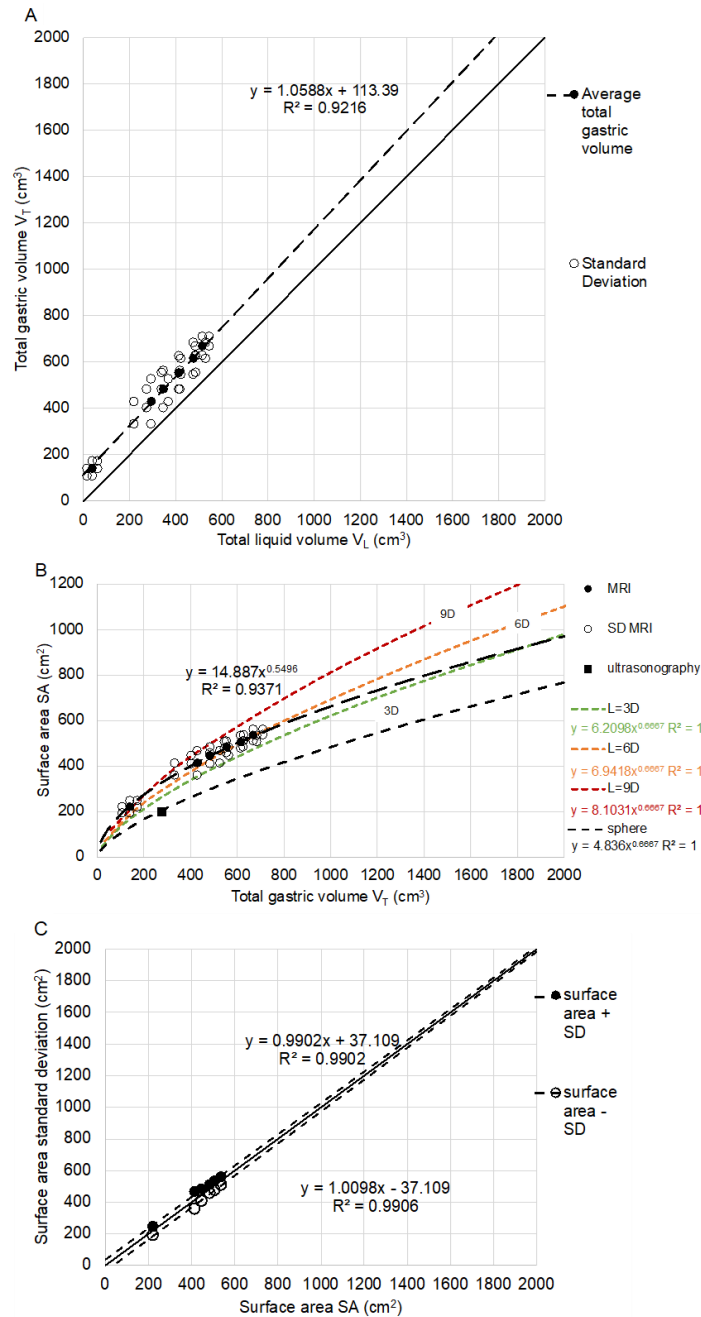


Figure 1. Changes in the in vivo volume (V_T), total liquid volume (V_L) and surface area (SA), with standard deviation (SD) values shown [11]. **A.** The change in V_T with $V_T > V_L$ due to the presence of $V_G + V_W$ (eq (1)). **B.** The change in the gastric SA values with V_T values from the MRI results (MRI, SD MRI) [11] compared to the SA/V values calculated for cylinders with $L=(3, 6, 9)$ D with the line of best fit as power equations. A single in vivo SA/V value from ultrasonography indicates a spherical shaped stomach as the SA/V data point is on the SA/V curve for a sphere which has the minimum possible SA/V ratio with $SA \approx 800 \text{ cm}^2$ when $V_T \approx 2000 \text{ cm}^3$ [8]. **C.**

The SD for the average SA values can be added or subtracted from the 6 SA values with the line of best fit used to obtain equations to calculate SD for $SA \approx 0-2000 \text{ cm}^2$. Data adapted from Bertoli et al. 2023 [1].

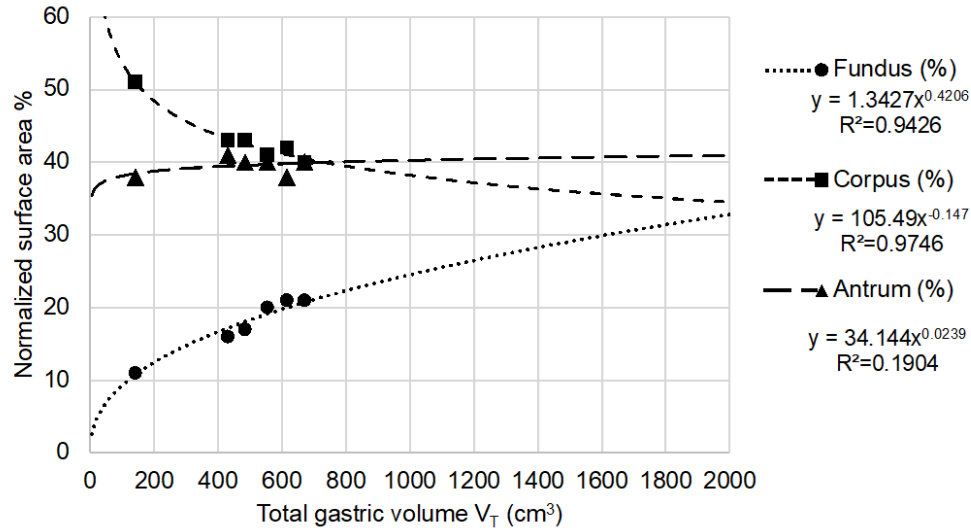


Figure 2. Normalized SA ratios (%) for 3 gastric regions for $V_T \approx 0-2000 \text{ cm}^3$ show the fundus expands with increasing V_T relative to the corpus, while the antrum remains relatively unchanged. Data adapted from Bertoli et al. 2023 [1].

Assigning 16 values for V_M between $V_M \approx 0-2000 \text{ cm}^3$ with $V_M \approx V_L$ (eq. (1)) and solving eq. (3), (4) (derived from the experimental values) generates V_T and SA values which can both be used in eqs. (8), (9) and on solving simultaneous, generating cylinder L and D values, Table 1. Solutions to the simultaneous equations give values for the cylinder $L \approx 26-28 \text{ cm}$ which do not increase continuously with increasing D values, with D increasing from $D \approx 2.4-10.3 \text{ cm}$, Table 1, Figure 3B.

If the cylinder L is extended to include the length to the centre of the circular top and base (L_{CTB}) of the cylinder, L now increases as part of the increasing diameter of the cylinder by $2r$, such that

$$L_{CTB} = L + 2r \quad (10)$$

with $L_{CTB} \approx 28-37 \text{ cm}$ at $D \approx 2.4-10.3 \text{ cm}$, Figure 3B.

If the cylinder is opened and flattened and includes the area of the circular cylinder caps, a new flat rectangular surface can be created with width (W) defined by the circumference (C):

$$W = C = 2\pi r = \pi D \quad (11)$$

with L now requiring an extend length (L_E) to include the additional length (L_A) from the circular top and base:

$$L_E = L + L_A \quad (12)$$

with the new flattened area ($L_A \times W$) equal to the area of the 2 circular caps ($2\pi r^2$):

$$L_A W = 2(\pi r^2) \text{ or } L_A = 2\pi r^2 / 2\pi r = r$$

such that:

$$L_E = L + r \quad (13)$$

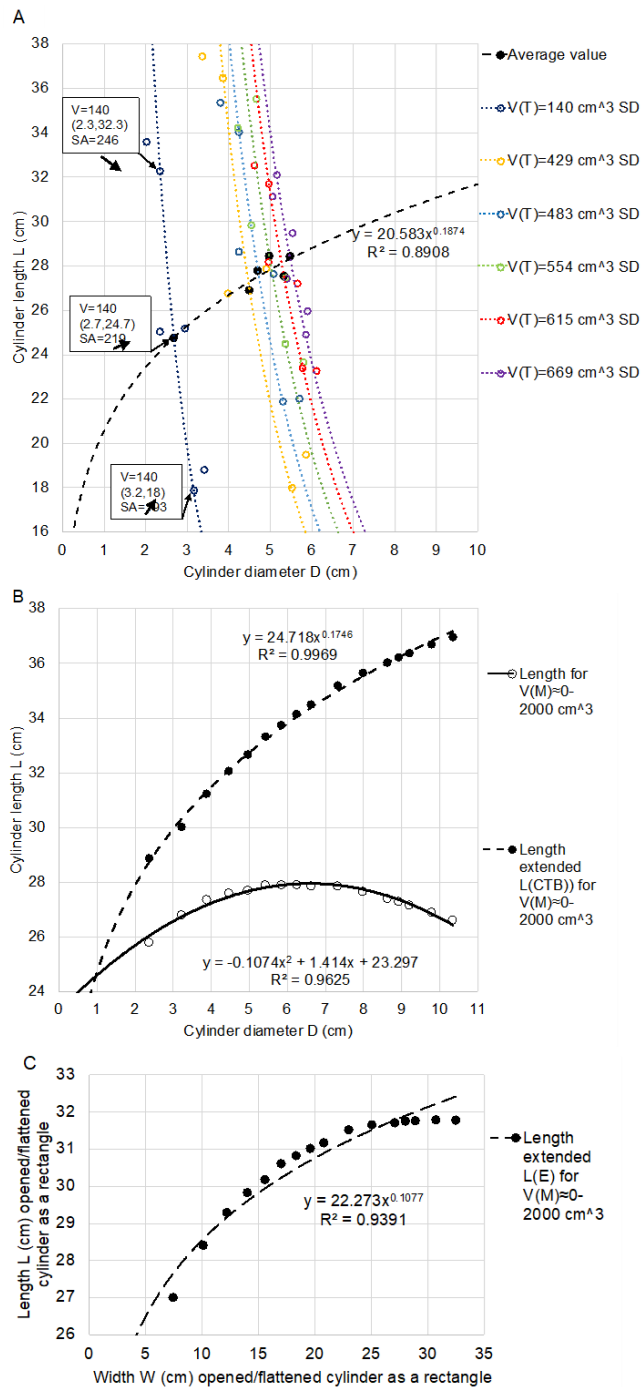


Figure 3. A. The 6 SA and V_T values including the SD values, from the MRI study are used in eqs. (8), (9) to form simultaneous equations which on solving give the L and D values [11]. For any given V_T value, multiple L and D values are possible generating multiple SA values as shown for $V = 140 \text{ cm}^3$ with D and L values expressed as (D, L) coordinates showing $SA \approx 193\text{--}246 \text{ cm}^2$ for $L \approx 18\text{--}32.3 \text{ cm}$ and $D \approx 2.3\text{--}3.2 \text{ cm}$, Figure 2A. The line of best fit only includes the 6 averaged V_T /SA values. **B.** From the 16 hypothetical $V_M \approx 0\text{--}2000 \text{ cm}^3$, calculated V_T and SA values from eqs. (3), (4) included in eqs. (8), (9) and solved simultaneously show an

almost constant value of $L \approx 26-28$ cm with $D \approx 2.4-10.3$ cm with L declining for $D \geq 6-7$ cm, Table 1. When both the cylinder caps radii are included in the L then it is extended by $2r$, the extend cylinder $L_{CTB} \approx 29-37$ cm show the expected increase with $D \approx 2.5-10.5$ cm. C. The cylinder can be opened and flattened to form a rectangle increasing L by r , with L_E increasing with W value, Table 1.

Meal Volume ($V_M \text{ cm}^3$)	Total gastric volume (V_T cm^3) eq. (3)	Surface area (SA cm^2) \pm SD eq. (4), (5)	Simultaneous eqs (8), (9)		Extended length (L_E cm) Circular opened to form a rectangle eqs. (12), (13)	Cylinder width (W cm) eq. (11)
			Cylinder height = length (L cm)	Cylinder diameter = $2r$ (D cm)		
0	113	200 \pm 37	25.8	2.37	27.0	7.45
100	219	288 \pm 36	26.8	3.22	28.4	10.1
200	325	359 \pm 35	27.35	3.88	29.3	12.2
300	431	418 \pm 34	27.6	4.46	29.8	14.0
400	537	472 \pm 33	27.7	4.96	30.2	15.6
500	643	521 \pm 32	27.9	5.42	30.6	17.0
600	749	566 \pm 31	27.9	5.84	30.8	18.3
700	855	609 \pm 30	27.9	6.24	31.0	19.6
800	961	649 \pm 29	27.9	6.62	31.2	20.8
1000	1173	725 \pm 27	27.9	7.32	31.5	23.0
1200	1385	794 \pm 25	27.7	7.98	31.65	25.1
1400	1597	858 \pm 23	27.4	8.62	31.7	27.1
1500	1703	889 \pm 22	27.3	8.92	31.75	28.0
1600	1809	919 \pm 21	27.2	9.2	31.8	28.9
1800	2021	977 \pm 19	26.9	9.78	31.8	30.7
2000	2233	1032 \pm 18	26.6	10.3	31.8	32.5

Table 1. Calculated values of V_T and SA from eqs. (3), (4) can be used in eqs. (8), (9) describing cylinder V and SA and solved simultaneously to give L and D values. The calculated L values do not show an increasing trend with V_M or V_T . On rolling out and flattening the cylinder to form a rectangle, the L values are adjusted to include the area from the cylinder caps, giving an extended length (L_E) at increasing V_M and V_T . The L_E and W multiplied together give a value for the SA of the stomach.

If the cylinder is opened and flattened and includes the area of the circular cylinder caps, a new flat rectangular surface can be created with width (W) defined by the circumference (C):

$$W = C = 2\pi r = \pi D \quad (11)$$

with L now requiring an extend length (L_E) to include the additional length (L_A) from the circular top and base:

$$L_E = L + L_A \quad (12)$$

with the new flattened area ($L_A \times W$) equal to the area of the 2 circular caps ($2\pi r^2$):

$$L_A W = 2(\pi r^2) \text{ or } L_A = 2\pi r^2 / 2\pi r = r$$

such that:

$$L_E = L + r \quad (13)$$

with $r=D/2$ resulting in $L_E \approx 27\text{--}32$ cm and $W \approx 7.5\text{--}32.5$ cm for $V_M \approx 0\text{--}2000$ cm³, Figure 3C, Table 1. Note L_{CTB} was extended by $2r$ for the cylinder while L_E for the rolled and flattened cylinder to form a rectangular shape, was only extended by r .

The maximum $L_{CTB} \approx 37$ cm and $L_E \approx 32$ cm for the cylinder model were comparable to the maximum greater curvature values for J shaped stomachs, with $L \approx 30\text{--}34$ cm, which includes both the length and radius of the stomach at $D \approx 10$ cm [3][6].

Approximations and limitations

Modelling changes of stomach SA with V in vivo is a complex process and it is not surprising few results are available and over a limited ranges of V [1][8]. Any model developed to describe the stomach requires many approximations including the shape, stomach wall thickness, what points to use for the measurement of L, D and the greater or lesser curvatures values, due to a lack of precise anatomical boundaries [1][3][6]. In this study, the main approximation was that the trends in SA and V values measures from consuming $V_M \approx 500$ cm³ of soup, could be extended to $V_M \approx 500\text{--}2000$ cm³ [1].

Conclusion

Equations have been developed to allow the calculation of the SA of the stomach in vivo for any given V_M . For SA ≈ 200 – 1030 cm^2 at $V_M \approx 0$ – 2000 cm^3 with a cylindrical model, when opened and flattened to form a rectangle, showing $L \approx 27$ – 32 cm with $W \approx 7.5$ – 32 cm . The cylinder model also shows that for any given V , by changing L and D , multiple values for the SA are possible, indicating that the stomach, by changing shape, changes SA.

Conflict of interest: The author declares no conflict of interest.

Data availability: All data is available from the references or contained within.

References

1. Bertoli D, Mark EB, Liao D, Brock C, Frøkjær JB, Drewes AM. A novel MR I-based three-dimensional model of stomach volume, surface area, and geometry in response to gastric filling and emptying. *Neurogastroenterol Motil.* 2023;35:e14497.
2. Hurr TJ. The consumption of iceberg lettuce may reduce the adhesion of dietary fat to the mucus surface of the stomach barrier lining decreasing the risk of triggering acute gastroesophageal reflux. *bioRxiv* 2023.08.26.554975; doi: <https://doi.org/10.1101/2023.08.26.554975>
3. Brandstaeter S, Fuchs SL, Aydin RC, Cyron CJ. Mechanics of the stomach: A review of an emerging field of biomechanics. *GAMM - Mitteilungen* 2019;42:e201900001.
4. Karnul AM, Murthy CK. A study of variations of the stomach in adults and growth of the fetal stomach. *Cureus.* 2022;14:e28517.
5. Monica YN, Somasekar R, Narasamma KC, Jayamma CH, Vanisree SK, Rajaneesh L, Prashanti T, Punarjeev an M, Reddy M. Anatomy of stomach and its variations. (*IOSR-JDMS*) *J Dental Med Sci.* 2020;19:55–61.
6. Ferrua MJ, Fanbin KR, Singh RP. Computational modeling of gastric digestion and the role of food material properties. *Trends in Food Science & Technology.* 2011;22:480–491.
7. Susmallian S, Goitein D, Barnea R, Raziel A. Correct evaluation of gastric wall thickness may support a change in staplers' size when performing sleeve gastrectomy. *IMAJ.* 2017;19:351–354.
8. Liao D, Gregersen H, Hausken T, Gilja OH, Mundt M, Kassab G. Analysis of surface geometry of the human stomach using real-time 3-D ultrasonography in vivo. *Neurogastroenterol Motil.* 2004;16:315–24.

Declarations

Funding: No specific funding was received for this work.

Potential competing interests: No potential competing interests to declare.